Nucleon-induced fragment formation with antisymmetrized molecular dynamics

Yoshiharu Tosaka
Fujitsu Laboratories Ltd., 10-1 Morinosato-Wakamiya, Atsugi 243-0197, Japan

Akira Ono
Department of Physics, Tohoku University, Sendai 980-77, Japan

Hisashi Horiuchi
Department of Physics, Kyoto University, Kyoto 606-01, Japan
(Received 16 December 1998; published 16 November 1999)

The 180 MeV $p+^{27}$Al reaction is investigated using antisymmetrized molecular dynamics, i.e., AMD and AMD-V, to investigate properties of fragment formations in medium energy nucleon-induced reactions. After statistical decay calculations, both AMD and AMD-V almost reproduce experimental mass distributions, differential, and double differential spectra of fragments in the $p+^{27}$Al reaction. However, the inclusion of the diffusion and the deformation of wave packets in AMD-V has drastic effects and, then, aspects in dynamical calculations of AMD-V are very different from AMD calculations. It is shown that various aspects of nucleon-induced reactions, in which residual nuclei decay into several fragments, appear in AMD-V calculations. The decay into fragments proceeds slowly, and thus, differs from the multiple fragmentation in heavy ion collisions. The possibility that AMD-V dynamical calculations describe the processes of statistical decays is discussed. [S0556-2813(99)03511-6]

PACS number(s): 25.40.−h, 25.70.Mn, 25.70.Pq, 24.90.+d

I. INTRODUCTION

Recently, quantum-mechanical molecular-dynamics models of nuclear reactions have made remarkable progress and have been applied to various kinds of reactions, especially heavy ion collisions [1–8]. Antisymmetrized molecular dynamics (AMD) is one of these models [4–6]. Because the nuclear system is described by a Slater determinant, AMD satisfies Pauli's principle and, therefore, is suitable for investigating quantum effects, for example, the clustering effect [9] in heavy ion collisions. AMD has been successfully applied to explaining fragment formations, nucleon and fragment flow, and so on, in heavy ion collisions.

Although AMD was most powerful for heavy ion collisions among the models that had ever been proposed, it was extended to include the effects of the diffusion and/or the deformation of the wave packets. This extended version was called AMD-V and was applied to heavy ion collisions [7], [8]. The extension of AMD gave the drastic effects of producing multiple fragments and led to a better reproduction of measured data.

AMD and AMD-V have been applied to heavy ion collisions and their high applicability has been demonstrated, but their application to light ion reactions has been very limited except for the work of Refs. [10] and [11]. In Ref. [10], they investigated medium energy $(p,p'x)$ reactions of 120 MeV $p+^{58}$Ni and of 90 MeV and 200 MeV $p+^{12}$C reactions using AMD and discussed two- and three-step contributions to angular distributions. However, the study of light ion induced fragmentation with AMD and AMD-V has made little progress and more detailed investigations are desired. The purpose of this paper is to investigate the properties of fragment formation in nucleon-induced reactions by using both AMD and AMD-V. Chiba *et al.* investigated the nucleon-induced fragmentation in the high-energy region (greater than 1 GeV) using quantum molecular dynamics (QMD) and showed that QMD well reproduced the measured mass distributions in 1.5 GeV $p+^{56}$Fe reactions [12]. On the other hand, we focus on the nucleon-induced fragmentation in the medium energy region in this paper.

We apply AMD and AMD-V to $p+^{27}$Al reaction with a proton incident energy of 180 MeV [13]. The fragmentation data in medium energy nucleon-nucleus reactions are very limited except for this reaction. The results of AMD and AMD-V are compared to experimental mass distribution, and to differential and double differential spectra of fragments in the $p+^{27}$Al reaction. It will be shown that both AMD and AMD-V reproduce this data after statistical decay calculations but aspects of the dynamical calculation by AMD-V are very different from those by AMD. Effects of the inclusion of the diffusion and the deformation of wave packets in AMD-V are found to be drastic. It will be shown that various aspects of nucleon-induced reactions, in which residual nuclei decay into several fragments, appear in AMD-V calculations. These decaying phenomena proceed slowly and, thus, differ from the multiple fragmentation in heavy ion collisions. The possibility that AMD-V dynamical calculations describe the time evolution in processes of statistical decays will be also discussed.

The contents of this paper are as follows. In Sec. II, formulations of AMD and AMD-V are given, and then in Sec. III, calculated results of AMD and AMD-V are described in detail. Section IV is devoted to the discussion of the characteristics of AMD and AMD-V for nucleon-induced reactions. A summary is given in Sec. V.

II. ANTISYMMETRIZED MOLECULAR DYNAMICS (AMD)

A. Usual AMD

The AMD wave function for the A-nucleon nuclear system is described by a single Slater determinant in which single-particle wave functions are expressed as Gaussian wave packets:

$$|\Phi(\mathbf{Z})\rangle = \det\left[\exp\left[-\nu\left(\mathbf{r}-\frac{\mathbf{Z}_\mathrm{i}}{\sqrt{\nu}}\right)^2+\frac{1}{2}\mathbf{Z}_\mathrm{i}^2\right]\chi_{\alpha_\mathrm{i}}\right]. \quad (1)$$

The complex variables $Z\equiv\{\mathbf{Z}_i\}$ are the centroids of the wave packets. α_i represents the spin-isospin label of the single-particle state and χ is the spin-isospin wave function. We took the width parameter $\nu=0.16$ fm^{-2}. An equation of motion which is derived from the time-dependent variational principle determines the time evolution of Z and is given by

$$i\hbar\sum_{j\tau} C_{i\sigma,j\tau}\dot{Z}_{j\tau}=\frac{\partial H}{\partial Z_{i\sigma}^*}, \quad (2)$$

where $C_{i\sigma,j\tau}$ with $\sigma,\tau=x,y,z$ is a Hermitian matrix

$$C_{i\sigma,j\tau}=\frac{\partial^2}{\partial Z_{i\sigma}^*\partial Z_{j\tau}}\ln\langle\Phi(\mathbf{Z})|\Phi(\mathbf{Z})\rangle. \quad (3)$$

H is the expectation value of the Hamiltonian after the subtraction of the spurious kinetic energy of the zero-point oscillation of the center of masses of fragments,

$$H(\mathbf{Z})=\frac{\langle\Phi(\mathbf{Z})|\mathsf{H}|\Phi(\mathbf{Z})\rangle}{\langle\Phi(\mathbf{Z})|\Phi(\mathbf{Z})\rangle}-\frac{3\hbar^2\nu}{2M}A+T_0[A-N_F(\mathbf{Z})], \quad (4)$$

where $N_F(\mathbf{Z})$ is the fragment number and T_0 is treated as a free parameter for the adjustment of the binding energies. In order to incorporate the two-nucleon collision processes due to residual interaction, the physical coordinates $W\equiv\{\mathbf{W}_i\}$ are introduced by

$$\mathbf{W}_i=\sum_{j=1}^{A}(\sqrt{Q})_{ij}\mathbf{Z}_j, \quad Q_{ij}=\frac{\partial}{\partial(\mathbf{Z}_i^*\cdot\mathbf{Z}_j)}\ln\langle\Phi(\mathbf{Z})|\Phi(\mathbf{Z})\rangle. \quad (5)$$

In AMD simulations for nucleus-nucleus collisions, the ground state of the nucleus is obtained by the cooling method. The dynamical process is then simulated by following the equation of motion, in which two-nucleon collision processes due to the residual interaction are stochastically incorporated using the physical coordinates of Eq. (5). In this paper, we adopted the Gogny force [14] as an effective interaction and the free cross section [10] as a two-nucleon collision cross section. We assumed the impact parameter (bimp) of less than 6 fm in AMD (and AMD-V) simulations for the $p+^{27}$Al reaction. To get the final distribution of fragments, we used an additional code [2] for statistical decay calculations which is similar to CASCADE by Pühlhofer [15].

In another molecular-dynamics approach [16], a fragment recognition procedure is applied at an early time in order to get rid of the unreliable time evolution of the molecular dynamics in the late stage. On the other hand, in the present work, we try to describe the fragmentation reaction by the dynamical model as much as possible by continuing the AMD calculation for a sufficiently long time. The statistical decay calculation is applied to the equilibriated fragments whose decay should take a long time physically.

B. AMD-V

The AMD-V is a modified version of AMD and is constructed by the stochastic incorporation of the diffusion and the deformation of wave packets which is calculated by the Vlasov equation. The Vlasov equation is given by

$$\frac{\partial f_\mathrm{i}}{\partial t}+\frac{\partial h}{\partial\mathbf{p}}\cdot\frac{\partial f_\mathrm{i}}{\partial\mathbf{r}}-\frac{\partial h}{\partial\mathbf{r}}\cdot\frac{\partial f_\mathrm{i}}{\partial\mathbf{p}}=0, \quad (6)$$

where h is the Wigner representation of a single-particle Hamiltonian calculated with an AMD wave function and f is the one-body distribution function for one nucleon and is represented by the Gaussian function,

$$f_\mathrm{i}(x,t_0)=F(x-X_\mathrm{i}(t_0)), \quad F(x)=\prod_{\alpha=1}^{6}\sqrt{2/\pi}\mathrm{e}^{-2x_\alpha^2}, \quad (7)$$

where variables x and X are given as follows:

$$x=\{x_\alpha\}_{\alpha=1,\ldots,6}=\{\sqrt{\nu}\mathbf{r},\mathbf{p}/2\hbar\sqrt{\nu}\}, \quad (8)$$

$$X_i=\{X_{i\alpha}\}_{\alpha=1,\ldots,6}=\{\mathbf{W}_i\}=\{\sqrt{\nu}\mathbf{R}_i,\mathbf{P}_i/2\hbar\sqrt{\nu}\}. \quad (9)$$

In order to reflect the Vlasov equation in AMD, we take the following stochastic procedure for the short time step between t_0 and $t_0+\delta t$. At $t=t_0$, the one-body distribution function is given by Eq. (7). At $t=t_0+\delta t$, the one-body distribution function is written as a superposition of Gaussian functions,

$$f_i(x,t_0+\delta t)=(1-c)F(x-X_i(t_0+\delta t))+c\int \mathrm{g}(\xi)F(x-X_i(t_0+\delta t)-\xi)d\xi. \quad (10)$$

By this expression, the diffusion and the deformation of wave packets are stochastically incorporated. A parameter c and a function g are determined by solving the Vlasov equation. In this procedure, the adjustment of the energy conservation and the Pauli principle are incorporated properly. More detailed descriptions of AMD-V are given in Ref. [7].

There are several works that extended the molecular dynamics by treating the wave-packet widths as deterministic dynamical variables [3,17–19]. Although this extension can be an improvement for some phenomena [17], it does not work well for fragmentation phenomena because the diffused wave packets will not shrink again to form fragments [18], [19] in a hot and expanding system. On the other hand, in

our stochastic treatment of the wave-packet diffusion effect, the fragmentation is well described since the dynamics chooses one of the possible fragmentation channels stochastically [7,20].

C. Preparing ground state of target nucleus

In the first stage of AMD and AMD-V simulations for nucleon-nucleus reactions, the ground state of the target nucleus is prepared using the cooling method. The equation for this method is introduced by multiplying a complex factor $\lambda+i\mu$, $\mu<0$, to the right-hand side of the AMD equation of motion of Eq. (2). If the system follows this cooling equation, the energy decreases with time. Starting with randomly chosen **Z** and solving this cooling equation, we reach the ground state of the nucleus. The validity of this method for describing ground states of nuclei was shown in Ref. [4]. However, we should note that the state of local minimum energy, which is not the ground state, may be obtained from cooling simulations. The ^{27}Al is just as a such case.

We applied this method to the ^{27}Al nucleus and obtained two different states. Because of their values of deformation parameters β and γ, one has an oblate shape (STATE 1) and the other has a prolate shape (STATE 2). We chose STATE 1 as the ground state. The binding energy of STATE 1 is lower by about 5 MeV than that of STATE 2 and reproduces the experimental value of -225 MeV. It is known that Hartree-Fock calculations give an oblate deformation for stable nuclei around $A=28$. The oblate shape of STATE 1 is rather exotic and seems to have a $t+2\alpha+^{16}$O cluster structure (which will be seen in Fig. 3(a)).

III. RESULTS

A. Time evolution of reactions

We first describe the features of the time evolution of the reaction. Figures 1 and 2 are examples of the time evolution of the density projected onto the reaction plane. Figures 1(a) and 1(b) show the results of AMD simulations with bimp = 1.0 fm and 4.7 fm, respectively, and Figs. 2(a) and 2(b) show the results of AMD-V simulations with bimp = 1.0 fm and 4.5 fm, respectively. In the case of the AMD results, a few nucleons are emitted after a proton incidence and after about 80 fm/c, the change of a residual nucleus, which is slightly deformed, is very slight with the time. On the other hand, in AMD-V, results drastically differ from AMD results. After a proton incidence, a residual nucleus is greatly deformed, and splits into two fragments with bimp = 1.0 fm and four fragments with bimp = 4.5 fm. Figures 3(a) and 3(b) show other examples of AMD-V simulations with bimp = 0.0 and 4.0 fm, respectively. In the case of bimp = 0.0 fm, 5 nucleons are emitted after a proton incidence and a residual nucleus is greatly deformed after nucleon emissions. It seems that the nucleon emissions in this example correspond to the statistical evaporation process. On the other hand, residual nucleus splits into two large fragments in the case of bimp = 4.0 fm.

Because the width of single-particle Gaussian wave packets in AMD wave functions is fixed, the AMD wave function cannot describe the large deformation and the splitting of

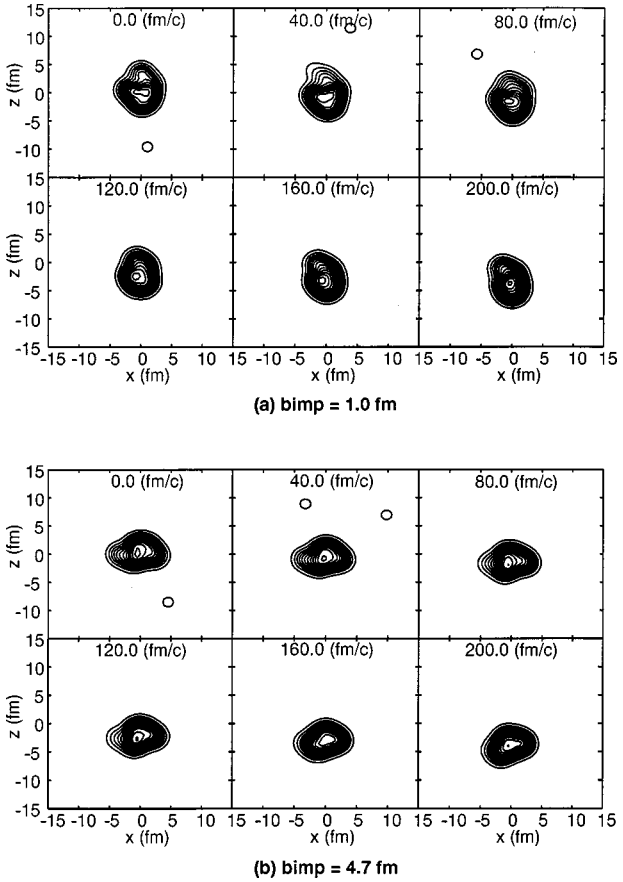

FIG. 1. Examples of the time evolution of the density projected onto the reaction plane from $t=0$ fm/c to 300 fm/c in a 180 MeV $p+^{27}$Al reaction. The calculated results with AMD are shown for impact parameters (a) bimp = 1.0 fm and (b) bimp = 4.7 fm.

wave packets even though the nucleus is highly excited. Then, AMD has the characteristic that the nucleus hardly decays in dynamical calculations. It seems that this characteristic is very prominent in this reaction compared to other heavy ion collisions [7]. On the other hand, effects of the improvement in AMD-V, which are the inclusion of the effects of diffusion and the deformation of wave packets, drastically appear in this reaction. However, these decaying phenomena proceed more slowly than those of heavy ion collisions. For example, recent results of the central ^{197}Au $+^{197}$Au collision with $E/A=150$ MeV show that nuclei break up into many fragments before 100 fm/c in AMD-V simulations [8]. Therefore, the decaying phenomena in the $p+^{27}$Al reaction at 180 MeV differ from the multiple fragmentation in heavy ion collisions.

Figures 4(a) and 4(b) show the mass distributions of fragments in dynamical calculations with AMD and AMD-V. The results at times 120, 220, and 320 fm/c are shown. The change in mass distributions in AMD calculations is very slight. The characteristic of AMD that the nucleus hardly decays in dynamical calculations again appears prominently. AMD produces fragments only of $A=1$ and 23–27. On the other hand, the effect of the improvement of including the deformation and the diffusion of wave packets appears in AMD-V calculations. At $t=120$ fm/c, fragments of $A=1$,

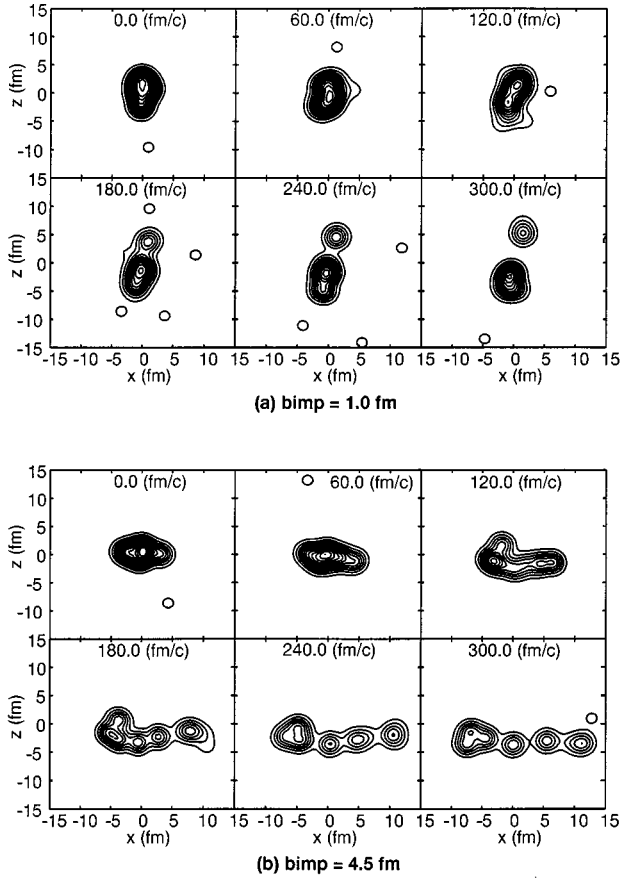

FIG. 2. Examples of the time evolution of the density calculated with AMD-V in the 180 MeV $p+^{27}$Al reaction are shown for impact parameters (a) bimp = 1.0 fm and (b) bimp = 4.5 fm.

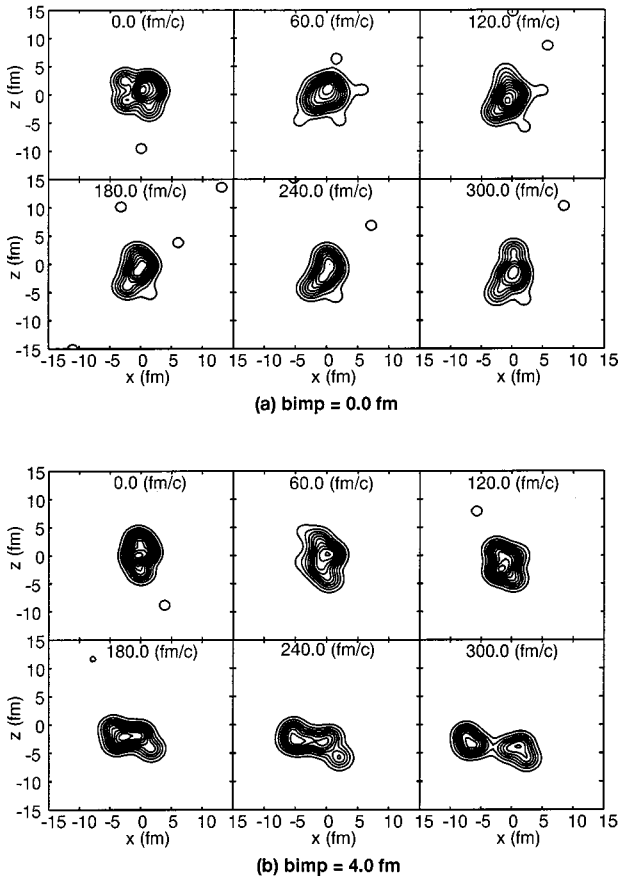

FIG. 3. Other examples of the time evolution of the density calculated with AMD-V in the 180 MeV $p+^{27}$Al reaction are shown for impact parameters (a) bimp = 0.0 fm and (b) bimp = 4.0 fm.

2, 4, 18, and 21–27 are already generated, during $t=120$ fm/c and 220 fm/c, fragments of $A=12-20$ are generated in addition, and most kinds of fragments are generated up to $t=320$ fm/c.

Figure 5 shows the internal energy per nucleon of the matter part of the system, which is defined as

$$\left(\frac{E}{A}\right)_{\text{matter}}=\frac{\sum_{k;A_k\geqslant 5}E_k}{\sum_{k;A_k\geqslant 5}A_k}, \tag{11}$$

where k is the label of the fragments in all events. A_k and E_k are the mass number and the internal energy of the fragment respectively, and the sum is taken for fragments with A greater than 4. The internal energy in AMD calculations does not change with time. On the other hand, it decreases slightly in AMD-V calculations. For comparison we also plotted the results of the ^{40}Ca+^{40}Ca reaction calculated by Ono *et al.* [7]. It can be understood that the 180 MeV $p+^{27}$Al reaction is an example of low internal energies and, therefore, decaying phenomena proceed very slowly.

B. Comparison with data and with other models

Figures 6(a) and 6(b) show the mass distribution of fragments calculated with AMD and AMD-V. Dotted lines show the results of dynamical calculations at $t=320$ fm/c and solid lines show the results after statistical decay calculations. In AMD calculations, most kinds of fragments are generated by statistical decay calculations. The mass distribution after statistical decay calculations has a similar shape as that of dynamical calculations for fragments of $A\leqslant 25$ in AMD-V. The mass distributions after statistical decay calculations are compared with the experimental data in Fig. 7(a). The difference between results of AMD and those of AMD-V is small and both results almost agree with experimental data, but the results of AMD-V agree slightly better than the results of AMD especially for fragments of $A=8-12$ and 23–26.

Results of QMD [21] are also shown in Fig. 7(b) for comparison. In the QMD calculations, the Skyrme-type interaction with parameters of the hard and the soft equation of state and the Pauli potential were used. Detailed descriptions of QMD are given in Refs. [22,23]. In dynamical calculations, QMD produces more kinds of fragments ($A=1-6$ and 17–27) but it gives rather similar results to AMD. After statistical decay calculations, QMD reproduces the experimental data for fragments of $A=16-27$. However, it largely underestimates the cross sections for fragments of $A=6-11$.

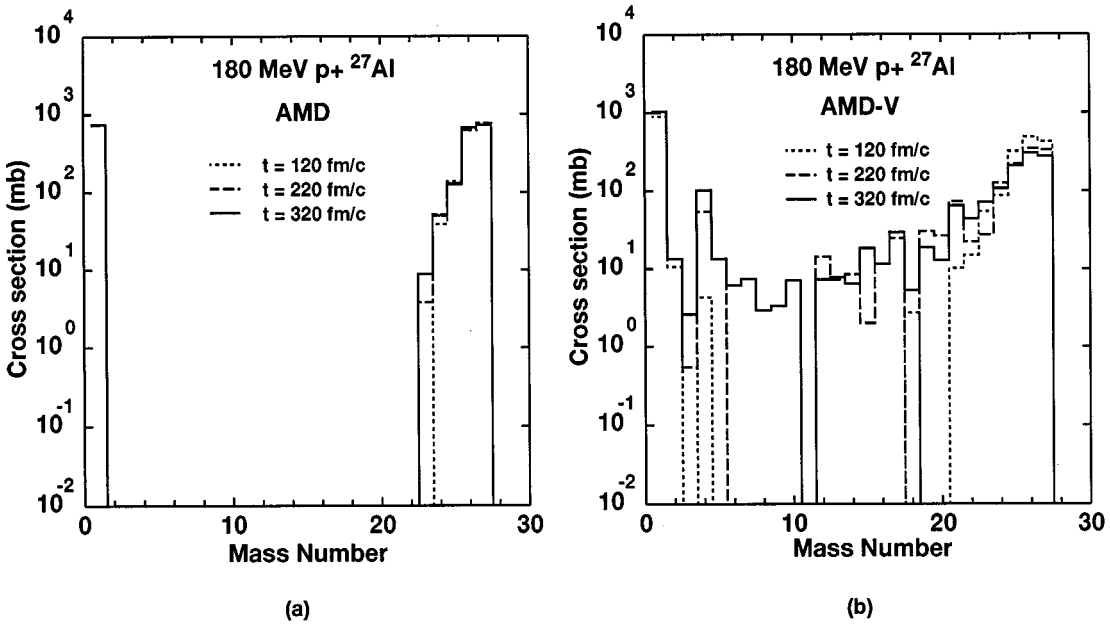

FIG. 4. Mass distribution of fragments at $t=120$, 220, and 320 fm/c in dynamical calculations with (a) AMD and (b) AMD-V.

Figure 8 shows double differential spectra of residual $A=22$ nuclei. Although both AMD and AMD-V underestimate the spectra in the high-energy region, they agree well with the experimental data in the energy range of less than 15 MeV. Although the difference between the results of the two models is small, it seems that AMD-V reproduces the gradient of a cross section curve for 20° slightly better than AMD. Figures 9(a) and 9(b) show differential spectra of residual nuclei of $A=12$, 16, 22, and 24. In the case of $A=24$, both models somewhat overestimate the spectra, but AMD-V gives slightly better results than AMD. In the case of $A=22$, the production cross sections by both models agree with the experimental values. It seems that the AMD-V reproduces the gradient of a cross section curve slightly better than AMD. In the case of $A=12$ and 16, both models somewhat underestimate the spectra, but AMD-V closely approximates the gradient of a cross section curve for $A=12$.

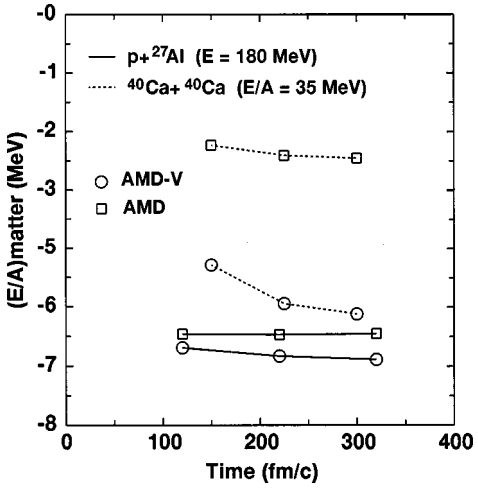

FIG. 5. Internal energy per nucleon of the matter part of the system in events as a function of the time in the dynamical calculation of AMD (squares) and AMD-V (circles) for the 180 MeV $p+^{27}$Al reaction. The results of the ^{40}Ca+^{40}Ca collision with energy of $E/A=35$ MeV [7] are also shown (dotted lines) for the comparison.

Tang *et al.* have also calculated with differential and double differential spectra of fragments in the 180 MeV $p+^{27}$Al reaction by using the cascade + the statistical decay model and reproduced values close to our results [24]. Although they gave excellent agreement with experimental data by an improvement of the statistical decay model, the cascade model based on classical mechanics and, thus, physical contents in dynamical calculations were very different from our calculations.

IV. DISCUSSIONS

AMD has the characteristic that the nucleus hardly decays in dynamical calculations as mentioned in the previous section, but it gave similar results with AMD-V after statistical decay calculations (AMD-V gave slightly better results than AMD). The reason is that AMD properly estimates the excitation energy in residual nuclei, which plays a major role in reproducing fragments in statistical decay calculations. Therefore, if we need only final results (for example, the mass distributions, etc.), the use of AMD with the statistical decay model may be good enough for this purpose.

On the other hand, the aspects of the dynamical calculations of AMD-V are very different from AMD calculations. Decaying phenomena in AMD-V dynamical calculations proceed slowly and differ from multifragmentation in heavy ion collisions. It is considerable that the various aspects in AMD-V dynamical calculations may describe the time evolution in processes of statistical decays. To see this point, we investigated the yield of the first and second heaviest frag-

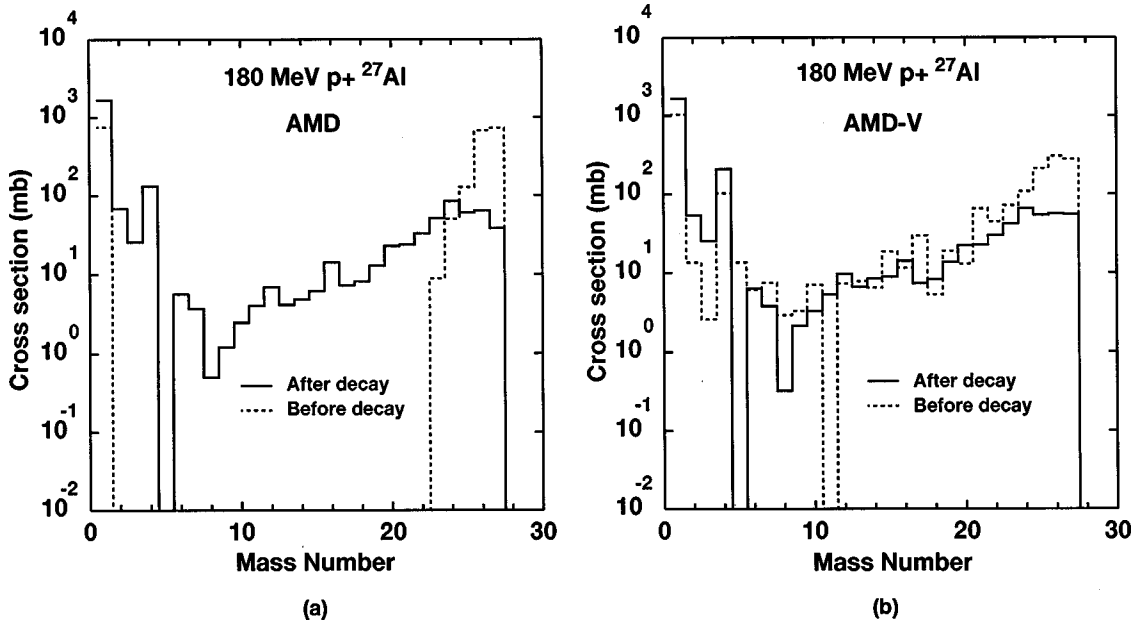

FIG. 6. Mass distribution of fragments at the end of the dynamical calculation (dotted histogram) and after the statistical decay calculation (solid histogram). The results of (a) AMD and (b) AMD-V are shown.

ments in each event [Figs. 10(a) and 10(b)]. In Figs. 10(a) and 10(b)], the areas of the boxes are proportional to the yield. After statistical decay calculations, both AMD and AMD-V give similar results. However, before statistical decay calculations, the results of AMD are very different from those of AMD-V. It seems that the distribution of boxes in AMD-V dynamical calculations is close to that of the final results and, thus, suggests that AMD-V can describe statistical decay processes.

We had to finish AMD-V dynamical simulations at 320 fm/c with 600 events, due to the calculation time limit. If we carry out dynamical calculations without the calculation time limit, AMD-V may reproduce the final results in Fig. 10(b) without statistical decay calculations. The new version of AMD-V, in which the triple loop approximation was used for estimating matrix elements, was recently proposed and demonstrated that it drastically reduced the calculation time [8]. Carrying out long duration and many event

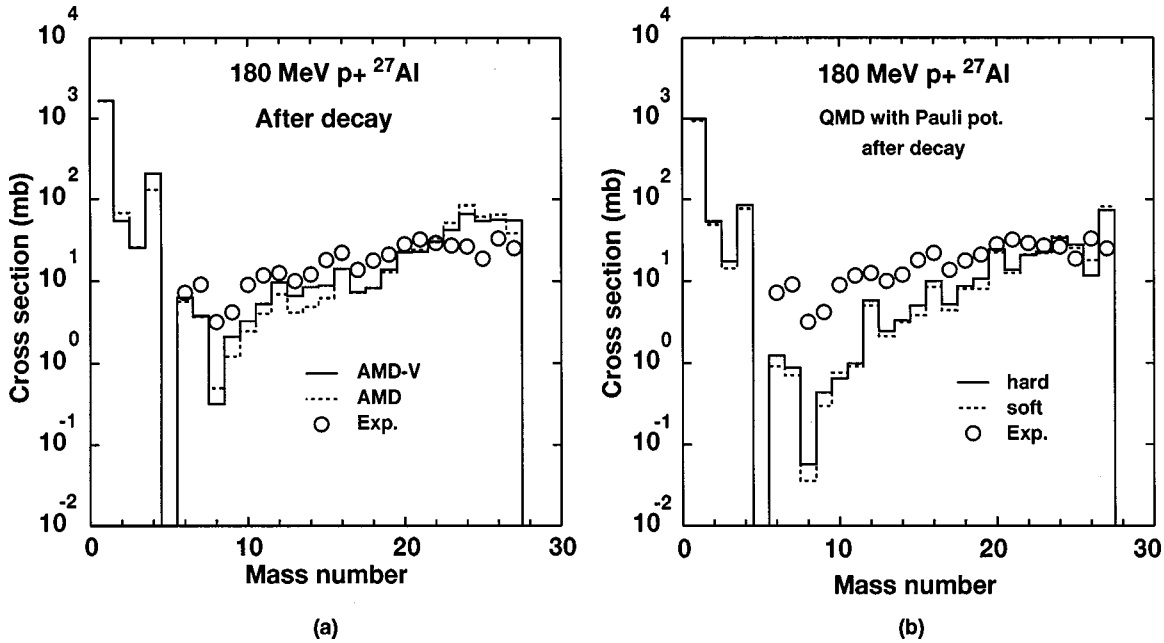

FIG. 7. (a) Mass distribution calculated with AMD (dotted histogram) and with AMD-V (solid histogram) after the statistical decay calculation compared with the experimental data (circles) [13]. The results of QMD + the statistical decay calculation [21] are also shown in (b) for the comparison. QMD results with parameter sets of the soft (dotted histogram) and the hard (solid histogram) equation of state are shown.

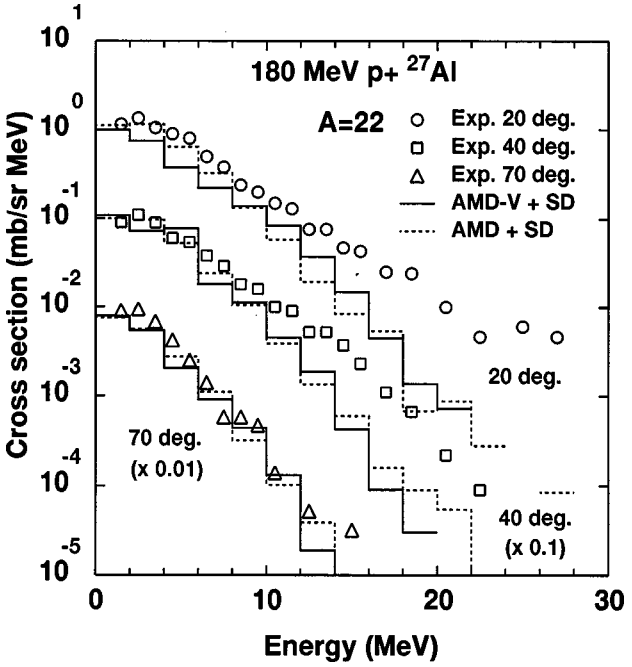

FIG. 8. Measured and calculated double differential cross sections for fragments with $A=22$ in the 180 MeV $p+^{27}$Al reaction. The results of AMD (dotted histogram) and AMD-V (solid histogram) are shown. The measured data are from Ref. [13].

simulations using the new AMD-V may be an interesting subject for the near future.

On the other hand, AMD-V dynamical reactions include some processes which conceptually differ from the statistical decay process and examples of such are actually shown in Figs. 2(b) and 3(b). It seems that the intermediate states of the residual nuclei in these events correspond to cluster structures in the well-known Ikeda diagram [25]. Various cluster structures with proper excitation energies in the Ikeda diagram may be found and the dynamics of the growth and the formation of cluster structures may be realized in AMD-V dynamical calculations. This suggests that we may find new physics in the various aspects of AMD-V dynamical reactions.

Furthermore, AMD and AMD-V are applicable for the soft error phenomena in VLSI electronics. Secondary cosmic ray neutrons induce soft errors in VLSI circuits at ground level through nucleon-induced reactions [26] and the importance of this phenomena was recently recognized [30,31]. The information of n nucleus (especially for $n+^{28}$Si) reactions with a medium neutron energy ($20\ \text{MeV} < \text{En} < 500$ MeV) is important for the accurate estimates of neutron-induced soft error rates. In this phenomena, heavy recoil nuclei which induce a large charge in a localized volume ($\sim 1\ \mu\text{m}^3$) in a silicon medium and, therefore, the simulation code which describes the nucleon-induced fragmentation is needed. Thus, AMD and AMD-V are suitable models for such applications.

V. SUMMARY

In this paper, we investigated the 180 MeV $p+^{27}$Al reaction using AMD and AMD-V to investigate properties of fragment formations in medium-energy nucleon-induced reactions.

After statistical decay calculations, AMD-V gave slightly better results than AMD but both models reproduced experimental mass distributions, and the differential and double differential spectra of fragments in the $p+^{27}$Al reaction.

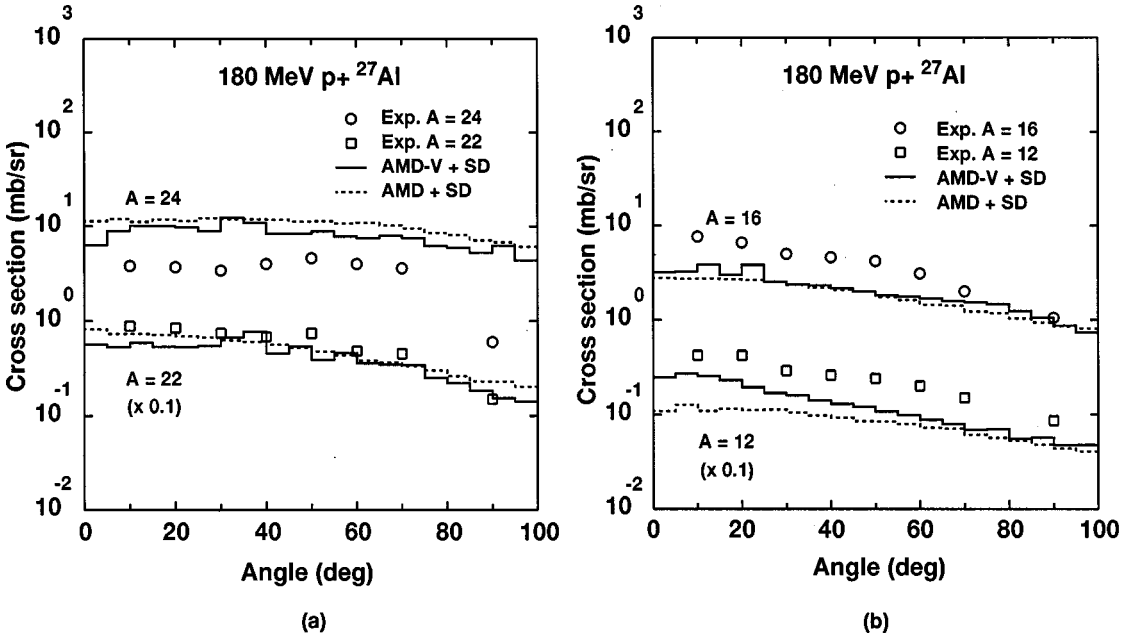

FIG. 9. Measured and calculated differential cross sections for fragments with (a) $A=24$ and 22 and with (b) $A=16$ and 12 in the 180 MeV $p+^{27}$Al reaction. The results of AMD (dotted histogram) and AMD-V (solid histogram) are shown. The measured data are from Ref. [13].

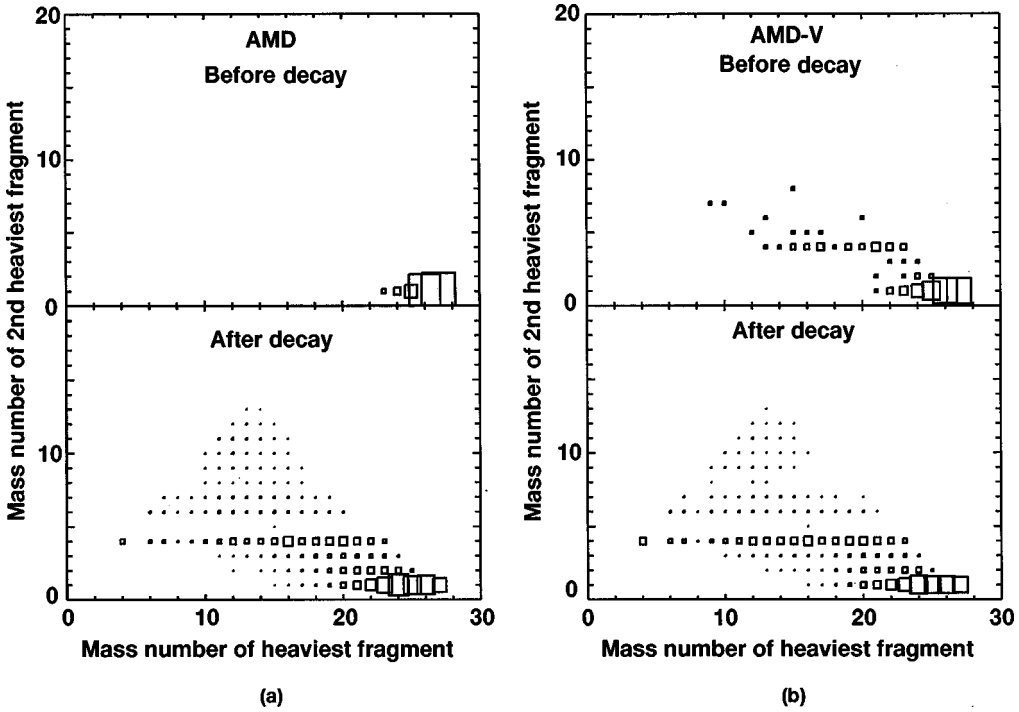

FIG. 10. Yield of pairs of first and second heaviest fragments in each event at the end of dynamial calculations (upper part) and after statistical calculations (lower part). The boxes are proportional to the yield. The results of (a) AMD and (b) AMD-V are shown.

Although both AMD and AMD-V gave similar results after statistical decay calculations, the aspects in dynamical calculations of AMD-V were very different from AMD calculations. The AMD wave function cannot describe the large deformation and the splitting of wave packets even though the nucleus is highly excited. This characteristic was very prominent in the 180 MeV $p+^{27}$Al reaction. On the other hand, the effects of the diffusion and the deformation of wave packets in AMD-V were found to be drastic. It was shown that various aspects of nucleon-induced reactions, in which residual nuclei decay into several fragments, appear in AMD-V calculations. These decaying phenomena proceed slowly, and thus differ from the multiple fragmentation in heavy ion collisions.

We investigated the yield of the first and second heaviest fragments in each event in AMD and AMD-V calculations and showed that the distribution of yields in AMD-V dynamical calculations close to that of final results after statistical decay calculations. It suggested that AMD-V dynamical calculations describe the time evolution in processes of statistical decays. Carrying out long duration and many event simulations to clarify this point using the new version of AMD-V with the triple loop approximation may be an interesting subject for the near future.

In the reaction studied here, the simultaneous multifragmentation did not take place since the excitation energy of the target nucleus is not sufficient. An interesting future subject is, therefore, to apply AMD and AMD-V to other reaction systems in which the excited nucleus can expand to low density. In this case, one of the possible fragmentation mechanisms is the spinodal decomposition [27–29], which should reflect the property of the nuclear matter in the low-density region.

ACKNOWLEDGMENTS

The authors thank Toshiki Maruyama of Japan Atomic Energy Research Institute for his kindness. He offered his results of QMD calculations of the 180 MeV $p+^{27}$Al reaction to us. Our work was carried out as a part of the research project for cosmic ray neutron-induced soft errors in Fujitsu Laboratories [30,31]. The authors thank S. Satoh, H. Kanata, K. Suzuki, T. Itakura, N. Nakayama, and N. Sasaki of Fujitsu Laboratory for their encouragement.

[1] J. Aichelin, Phys. Rep. **202**, 233 (1991).
[2] T. Maruyama, A. Ono, A. Ohnishi, and H. Horiuchi, Prog. Theor. Phys. **87**, 1367 (1992).
[3] H. Feldmeier, Nucl. Phys. **A515**, 147 (1990).
[4] A. Ono, H. Horiuchi, T. Maruyama, and A. Ohnishi, Phys. Rev. Lett. **68**, 2989 (1992); Prog. Theor. Phys. **87**, 1185 (1992).
[5] A. Ono, H. Horiuchi, T. Maruyama, and A. Ohnishi, Phys. Rev. C **47**, 2652 (1993).
[6] A. Ono and H. Horiuchi, Phys. Rev. C **51**, 299 (1995).
[7] A. Ono and H. Horiuchi, Phys. Rev. C **53**, 2958 (1996).
[8] A. Ono, H. Horiuchi, H. Takemoto, and R. Wada, Nucl. Phys. **A630**, 148 (1998); A. Ono and H. Horiuchi, *Proceedings of the XVII RCNP International Symposium on Innovative Computa-*

tional Methods in Nuclear Many-Body Problems, edited by H. Horiuchi *et al.* (World Scientific, Singapore, 1998), p. 443; A. Ono, nucl-th/9809029,
[9] H. Takemoto, H. Horiuchi, A. Engel, and A. Ono, Phys. Rev. C **54**, 266 (1996).
[10] E. I. Tanaka, A. Ono, H. Horiuchi, T. Maruyama, and A. Engel, Phys. Rev. C **52**, 316 (1995).
[11] A. Engel, E. I. Tanaka, T. Maruyama, A. Ono, and H. Horiuchi, Phys. Rev. C **52**, 3231 (1995).
[12] S. Chiba, O. Iwamoto, T. Fukahori, K. Niita, T. Maruyama, T. Maruyama, and A. Iwamoto, Phys. Rev. C **54**, 285 (1996).
[13] K. Kwiatkowski, S. H. Zhou, T. E. Ward, V. E. Viola, Jr., H. Breuer, G. J. Mathews, A. Gökmen, and A. C. Mignerey, Phys. Rev. Lett. **50**, 1648 (1983).
[14] J. Dechargé and D. Gogny, Phys. Rev. C **21**, 1568 (1980).
[15] F. Pühlhofer, Nucl. Phys. **A280**, 267 (1977).
[16] P. B. Gossiaux, R. Puri, Ch. Hartnack, and J. Aichelin, Nucl. Phys. **A619**, 379 (1997).
[17] Toshiki Maruyama, K. Niita, and A. Iwamoto, Phys. Rev. C **53**, 2958 (1996).
[18] D. Kiderlen and P. Danielewicz, Nucl. Phys. **A620**, 346 (1997).
[19] M. Colonna and Ph. Chomaz, Phys. Lett. B **436**, 1 (1998).
[20] A. Ono, Phys. Rev. C **59**, 853 (1999).
[21] T. Maruyama (private communication).
[22] T. Maruyama, K. Niita, T. Maruyama, and A. Iwamoto, Prog. Theor. Phys. **98**, 97 (1997).
[23] T. Maruyama, K. Niita, K. Oyamatsu, T. Maruyama, S. Chiba, and A. Iwamoto, Phys. Rev. C **57**, 655 (1998).
[24] H. K. Tang, G. R. Srinivasan, and N. Azziz, Phys. Rev. C **42**, 1598 (1990).
[25] H. Horiuchi, K. Ikeda, and Y. Suzuki, Suppl. Prog. Theor. Phys. **52**, 89 (1972).
[26] J.F. Ziegler and W.A. Lanford, Science **206**, 776 (1979); J. Appl. Phys. **528**, 4305 (1981).
[27] G. F. Bertsch and P. J. Siemens, Phys. Lett. B **126**, 9 (1983).
[28] H. Heselberg, C. J. Pethick, and D. G. Ravenhall, Phys. Rev. Lett. **61**, 818 (1988).
[29] B. Jacquot, S. Ayik, Ph. Chomaz, and M. Colonna, Phys. Lett. B **383**, 247 (1996).
[30] Y. Tosaka, S. Satoh, T. Itakura, K. Suzuki, T. Sugii, H. Ehara, and G. A. Woffinden, IEEE Electron Device Lett. **EDL18**, 99 (1997).
[31] Y. Tosaka, S. Satoh, T. Itakura, H. Ehara, T. Ueda, G. A. Woffinden, and S. A. Wender, IEEE Trans. Electron Devices **ED45**, 1453 (1998).